

Molecular Charge Distribution, Core-Ionization Energies, and the Point-Charge Approximation

Leif J. Saethre,^{*,1a} Michele R. F. Siggel,^{*,1b} and T. Darrah Thomas^{*,1c}

Contribution from the Department of Chemistry, Institute of Mathematical and Physical Sciences, University of Tromsø, N-9000 Tromsø, Norway, Lawrence Berkeley Laboratory and Department of Chemistry, University of California, Berkeley, California 94720, and the Department of Chemistry and Center for Advanced Materials Research, Oregon State University, Corvallis, Oregon 97331-4003. Received November 2, 1990

Abstract: Charge distributions in molecules are frequently studied experimentally with core-ionization spectroscopy and analyzed in terms of a potential model that assigns point charges at the atomic centers. This point-charge model has been evaluated by extensive *ab initio* calculations and the use of Bader's partitioning algorithm of electron density. With ethene and the monohalogenated ethenes as examples, it is shown that the model cannot describe properly the charge distribution and potentials at the atomic centers. It is necessary to consider both a valence radius that varies with atomic charge and the nonspherical distribution of electrons around the atoms in the molecule. The rather small atomic charges derived from the analysis of core-ionization energies with a point-charge model result from ignoring this nonspherical nature of the charge distributions. A possible improvement on the traditional point-charge model is a multipole expansion. It is shown that it is necessary to carry such an expansion at least through the octupole terms to obtain a reasonably accurate description of *shifts* in potentials. For absolute potentials, even higher multipoles will be needed.

The idea of charge transfer from one atom to another when bonds form is fundamental to chemistry and is embodied in the concept of electronegativity. As a result, there have been many attempts to provide experimental and theoretical definition to the charge on an atom in a molecule. Among the theoretical approaches are those based on electronegativity, such as Pauling charges,² those based on partitioning the molecule in Hilbert space, such as Mulliken populations^{3,4} and natural orbital populations,⁵ and those based on integration of the electron density over suitable volumes of the molecule in real space, such as integrated Bader populations.⁶⁻⁸ All of these suffer from an arbitrariness about how charge is to be apportioned, and each has its particular disadvantages.

Pauling's approach is based on assignment of charges in a few simple molecules from their dipole moments and an empirical relationship between these charges and the electronegativities of the atoms. Since the relationship between charges centered on atoms and the dipole moment is not straightforward, Pauling charges can have only qualitative significance. The Mulliken procedure, which is simple to implement, gives results that are dependent on the basis set used for the calculations; moreover, a better basis set does not necessarily lead to more meaningful atomic populations.^{4,9} The natural orbital method is thought to be less basis set dependent than the Mulliken method. It is, however, like the Mulliken approach, based on orbitals, which are constructs of the quantum mechanical theory rather than observable quantities.

Table I. Atomic Charges for Ethene and Haloethenes from Integrated Bader Population Analyses^a

X	C(1)	C(2)	X(3)	H(4)	H(5)	H(6)
H	-0.045	-0.045	+0.022	+0.022	+0.022	+0.022
F	+1.082	-0.431	-0.778	+0.053	+0.033	+0.045
Cl	+0.329	-0.282	-0.245	+0.089	+0.044	+0.069
Br	+0.144	-0.288	-0.052	+0.090	+0.048	+0.065
I	-0.104	-0.214	+0.118	+0.092	+0.053	+0.064

^aC(1) is attached to the halogen in haloethenes. H(4) is attached to C(1), and H(5) is trans to the halogen.

The Bader integration method is based on the electron density, which is, at least in principle, an experimentally measurable quantity. If polarization functions are included in the basis set, then the dependence of the Bader populations on the basis set is small.^{10,11} In the limit of an excellent basis set one may expect that they will converge to a value approaching what could be obtained by experiment.¹² In the Bader scheme, the molecule is divided into basins, each containing one of the atoms. The boundaries of the basins begin at the saddle points of the charge distribution and follow the steepest descent of the charge distribution to infinity. The population and other moments of the charge distribution are obtained for each atom by integration of the charge density over the basin. The method has the disadvantage of requiring extensive computer time. It has, however, a number of theoretical merits, which have been discussed by Bader,⁶ and the practical advantages of producing not only a population to be assigned to each atom but also other moments of the charge distribution.

Bader's method has been criticized because it often gives atomic charges that seem unrealistically large. Examples are found in Table I, where we show Bader charges for ethene and the monohaloethenes.¹³ Particularly striking are the results for fluoroethene, where the charge on fluorine is -0.78 and that on the adjacent carbon +1.08. These are close to the values expected for a purely ionic bond and distinctly larger than would be predicted from other approaches. For example, the Pauling approach

(1) (a) University of Tromsø. (b) University of California. Current address: S.E.R.C. Daresbury Laboratory, Daresbury, Warrington WA4 4AD, U.K. (c) Oregon State University.

(2) Pauling, L. *The Nature of the Chemical Bond*, 2nd ed.; Cornell University Press: Ithaca, NY, 1948; p 69.

(3) Mulliken, R. S. *J. Chem. Phys.* **1955**, *23*, 1833.

(4) Hehre, W. J.; Radom, L.; Schleyer, P. v. R.; Pople, J. A. *Ab Initio Molecular Orbital Theory*; John Wiley and Sons: New York, 1986; pp 336-341.

(5) Reed, A. E.; Weinstock, R. B.; Weinhold, F. *J. Chem. Phys.* **1985**, *83*, 753.

(6) (a) Bader, R. F. W. *Acc. Chem. Res.* **1985**, *18*, 9. (b) Bader, R. F. W.; Nguyen-Dang, T. T.; Tal, Y. *Rep. Prog. Phys.* **1981**, *44*, 893.

(7) Biegler-Koenig, F. W.; Bader, R. F. W.; Tang, T. H. *J. Comput. Chem.* **1982**, *3*, 317.

(8) (a) Bader, R. F. W.; Nguyen-Dang, T. T. *Adv. Quantum Chem.* **1981**, *14*, 63. (b) Bader, R. F. W.; Larouche, A.; Carrol, M. T.; MacDougall, P.; Wiberg, K. B. *J. Chem. Phys.* **1987**, *87*, 1142. (c) Wiberg, K. B.; Bader, R. F. W.; Lau, C. D. *J. Am. Chem. Soc.* **1987**, *109*, 985.

(9) (a) Wiberg, K. B. *J. Am. Chem. Soc.* **1990**, *112*, 4177. (b) Grier, D. L.; Streitwieser, A., Jr. *J. Am. Chem. Soc.* **1982**, *104*, 3556. (c) Mulliken, R. S.; Politzer, P. *J. Chem. Phys.* **1971**, *55*, 5135.

(10) (a) Siggel, M. R. F.; Streitwieser, A., Jr.; Thomas, T. D. *J. Am. Chem. Soc.* **1988**, *110*, 8022. (b) Wiberg, K. B.; Bader, R. F. W.; Lau, C. D. *J. Am. Chem. Soc.* **1987**, *109*, 1001. (c) Stutchbury, N. C. J.; Cooper, D. L. *J. Chem. Phys.* **1983**, *79*, 4967.

(11) Bachrach, S. M.; Streitwieser, A. *J. Comput. Chem.* **1989**, *10*, 514.

(12) Breitenstein, M.; Dannöhl, H.; Meyer, H.; Schweig, A.; Seeger, R.; Seeger, U.; Zittlau, W. *Int. Rev. Phys. Chem.* **1983**, *3*, 335.

(13) The computational details of the calculations on which these results are based are discussed subsequently.

gives a partial ionic character of 0.47 for a C-F bond.² The corresponding Mulliken charges are +0.34 for carbon and -0.40 for fluorine; the natural orbital populations give charges of +0.19 and -0.37. Similar results on oxygenated compounds have recently been obtained by Bachrach and Streitwieser,¹¹ who found atomic charges derived from Bader's method to be significantly higher than those derived from Hilbert space partitioning schemes (Mulliken and natural orbital populations). However, they noted that the center of gravity of the electrons did not coincide with the nuclei and that there was a local dipole which counteracted the dipole given by the nucleus-centered atomic charges.

One of the experimental methods that have been used to determine charge distribution in molecules is core-ionization spectroscopy. Since the earliest experiments, it has been apparent that core-ionization energies correlate well with atomic charges, regardless of how they are determined.¹⁴ In the simplest approximations, quantitative relationships between core-ionization energies and atomic charges are based on a point-charge model, in which the molecular charge distribution is approximated as point charges located at the nuclei.

Before applying such a model, however, it is necessary to recognize that core-ionization energies, I , depend not only on the charge distribution in the neutral molecule but also on the charge rearrangement that occurs when a core electron is removed. Thus the shifts in core-ionization energy can be expressed as^{15,16}

$$\Delta I = \Delta V - \Delta R \quad (1)$$

where V is the potential¹⁷ at the site of the core electron in the un-ionized molecule and R is the lowering of the energy of the final state by rearrangement of electrons in response to the removal of the core electron. V reflects the charge distribution of the neutral molecule and Δ refers to a shift in the quantity between one molecule and another.

In general, one must find a way to correct for the relaxation energy before using core-ionization energies as a probe of the charge distribution. Several methods are available for this. Experimental approaches are based on combined measurements of core-ionization energies and either Auger kinetic energies or gas-phase acidities. From the theoretical point of view, ab initio calculations at a level sufficiently high to reproduce the experimental core-ionization energies can provide values of ΔV and ΔR . There have been a number of studies in which these experimental and theoretical methods have been used and compared.¹⁸⁻²⁵ The

Table II. Experimental and Theoretical Results for C(1) in Ethene and in the Haloethenes^a

X	ΔI		ΔV theor	Δq		
	exptl	theor		MPA	NBO	IBP
H	+290.82	+291.78	-400.49	-0.21	-0.42	-0.05
F	+2.61	+2.62	+2.39	+0.55	+0.72	+1.13
Cl	+1.53	+1.56	+1.99	+0.18	+0.18	+0.37
Br	+1.16	+1.15	+1.79	+0.06		+0.19
I	+0.59	+0.80	+1.69	-0.17		-0.06

^a Actual values are reported for ethene. Values for the haloethenes are reported as shifts relative to ethene. Energies in eV. C(1) is attached to halogen in haloethenes. MPA = Mulliken population analysis. NBO = natural (bonding) orbital analysis. IBP = integrated Bader population analysis.

results are generally in accord with expectations from other chemical evidence and there is good agreement between theory and experiment.

The potential shift, ΔV , or, if relaxation effects are ignored, the shift in core-ionization energy, ΔI , can be related to the charge distribution of the molecule via the point-charge model,²⁵⁻³⁴ mentioned above. This relationship can be expressed mathematically as

$$\Delta V_i = \Delta \left(q_i \left\langle \frac{1}{r_i} \right\rangle + \sum_{j \neq i} \frac{q_j}{R_{ij}} \right) \quad (2)$$

where i refers to the atom of interest, j refers to the other atoms in the molecule, and the q 's represent the charges on these atoms, R_{ij} is the distance between atom i and atom j and r_i is the valence radius of atom i . The term $\langle 1/r_i \rangle$ is usually treated as if it is independent of charge. The shift, Δ , is taken relative to some reference molecule. The summation of eq 2 is often referred to as the Madelung potential.

Frequently eq 2 either is dominated by the first term or can be reduced to an expression in which ΔV_i is proportional to q_i .³⁴ Such relationships provide the basis for the many correlations between core-ionization energies and atomic charges that have been reported. Atomic charges derived with eq 2 are found to be in more or less agreement with theoretical expectations.^{18,35,36}

(14) Siegbahn, K.; Nordling, C.; Fahlman, A.; Nordberg, R.; Hamrin, K.; Hedman, J.; Johansson, G.; Bergmark, T.; Karlsson, S.-E.; Lindgren, I.; Lindberg, B. *ESCA, Atomic, Molecular and Solid State Structure Studied by Means of Electron Spectroscopy*; Almqvist and Wiksell: Uppsala, 1967.

(15) (a) Wagner, C. D. *J. Electron Spectrosc. Relat. Phenom.* **1988**, *47*, 283. (b) Wagner, C. D. *Faraday Discuss. Chem. Soc.* **1975**, *60*, 291. (c) Davis, D. W.; Shirley, D. A. *J. Electron Spectrosc. Relat. Phenom.* **1974**, *3*, 137.

(16) Thomas, T. D. *J. Electron Spectrosc. Relat. Phenom.* **1980**, *20*, 117.

(17) V is defined here as the potential at the site of the core electron. In eq 1 it actually represents the potential energy of a unit positive charge at this site; this is the usual definition of V . If we use either atomic units or volts for potential and atomic units or electron volts for energy, then the two definitions of V are numerically equal.

(18) Saethre, L. J.; Thomas, T. D.; Gropen, O. *J. Am. Chem. Soc.* **1985**, *107*, 2581.

(19) Siggel, M. R. F.; Nolan, G. S.; Saethre, L. J.; Thomas, T. D.; Ungier, L. *J. Phys. Chem.* **1981**, *91*, 3969.

(20) Perry, W. D.; Jolly, W. L. *Chem. Phys. Lett.* **1973**, *23*, 529.

(21) (a) Siggel, M. R.; Thomas, T. D. *J. Am. Chem. Soc.* **1986**, *108*, 4360. (b) Nolan, G. S.; Saethre, L. J.; Siggel, M. R.; Thomas, T. D.; Ungier, L. *J. Am. Chem. Soc.* **1985**, *107*, 6463. (c) Aitken, E. J.; Bahl, M. K.; Bomben, K. D.; Gimzewski, J. K.; Nolan, G. S.; Thomas, T. D. *J. Am. Chem. Soc.* **1980**, *102*, 4873. (d) Ashe, A. J., III; Bahl, M. K.; Bomben, K. D.; Chan, W.-T.; Gimzewski, J. K.; Sittin, P. G.; Thomas, T. D. *J. Am. Chem. Soc.* **1979**, *101*, 1764. (e) Smith, S. R.; Thomas, T. D. *J. Am. Chem. Soc.* **1978**, *100*, 5459.

(22) (a) Yan, C. X.; Cavell, R. G. *J. Electron Spectrosc. Relat. Phenom.* **1987**, *42*, 49. (b) Sodhi, R. N.; Cavell, R. G. *J. Electron Spectrosc. Relat. Phenom.* **1986**, *41*, 1. (c) Cavell, R. G.; Sodhi, R. N. *S. J. Electron Spectrosc. Relat. Phenom.* **1986**, *41*, 25. (d) Venezia, A. M.; Cavell, R. G. *J. Chem. Phys.* **1986**, *84*, 4797. (e) Sodhi, R. N. S.; Cavell, R. G. *J. Electron Spectrosc. Relat. Phenom.* **1983**, *32*, 283.

(23) Asplund, L.; Kelfve, P.; Siegbahn, H.; Goscinski, O.; Fellner-Feldegg, H.; Hamrin, K.; Blomster, B.; Siegbahn, K. *Chem. Phys. Lett.* **1976**, *40*, 353.

(24) (a) Bahl, M. K.; Woodall, R. O.; Watson, R. L.; Irgolic, K. J. *J. Chem. Phys.* **1976**, *64*, 1210. (b) Bahl, M. K.; Watson, R. L.; Irgolic, K. J. *J. Chem. Phys.* **1978**, *68*, 3272.

(25) Banna, M. S.; Slaughter, A. R.; Mathews, R. D. *J. Electron Spectrosc. Relat. Phenom.* **1986**, *40*, 317.

(26) Fadley, C. S.; Hagström, S. B. M.; Klein, M. P.; Shirley, D. A. *J. Chem. Phys.* **1968**, *48*, 3779.

(27) Siegbahn, K.; Nordling, C.; Johansson, G.; Hedman, J.; Heden, P. F.; Hamrin, K.; Gelius, U.; Bergmark, T.; Werme, L. O.; Manne, R.; Baer, Y. *ESCA Applied to Free Molecules*; North-Holland: Amsterdam, 1969; pp 104-136.

(28) (a) Gelius, U. *Phys. Scr.* **1974**, *9*, 133. (b) Stucky, G. D.; Matthews, D. A.; Hedman, J.; Klasson, M.; Nordling, C. *J. Am. Chem. Soc.* **1972**, *94*, 8009. (c) Gelius, U.; Roos, B.; Siegbahn, P. *Chem. Phys. Lett.* **1970**, *4*, 471.

(29) (a) Jolly, W. L.; Perry, W. B. *J. Am. Chem. Soc.* **1973**, *95*, 5442. (b) Jolly, W. L.; Hendrickson, D. N. *J. Am. Chem. Soc.* **1970**, *92*, 1863.

(30) (a) Sham, T. K.; Perlman, M. L.; Watson, R. E. *Phys. Rev. B* **1979**, *19*, 539. (b) Chou, T. S.; Perlman, M. L.; Watson, R. E. *Phys. Rev. B* **1976**, *14*, 3248. (c) Friedman, R. M.; Hudis, J.; Perlman, M. L.; Watson, R. E. *Phys. Rev. B* **1973**, *8*, 2433. (d) Watson, R. E.; Hudis, J.; Perlman, M. L. *Phys. Rev. B* **1971**, *4*, 4139.

(31) (a) Dash, K. C.; Folkesson, B.; Larsson, R.; Mohapatra, M. J. *Electron Spectrosc. Relat. Phenom.* **1989**, *49*, 343. (b) Sundberg, P.; Andersson, C.; Folkesson, B.; Larsson, R. *J. Electron Spectrosc. Relat. Phenom.* **1988**, *46*, 85.

(32) Wertheim, G. K.; Cohen, R. L.; Creelius, G.; West, K. W.; Wernick, J. H. *Phys. Rev. B* **1979**, *20*, 860.

(33) (a) Carroll, T. X.; Shaw, R. W., Jr.; Thomas, T. D.; Kindler, C.; Bartlett, N. *J. Am. Chem. Soc.* **1974**, *96*, 1989. (b) Carroll, T. X.; Thomas, T. D. *J. Chem. Phys.* **1974**, *60*, 2186.

(34) Thomas, T. D. *J. Am. Chem. Soc.* **1970**, *92*, 4184.

(35) Davis, D. W.; Shirley, D. A.; Thomas, T. D. *J. Am. Chem. Soc.* **1972**, *94*, 6565.

However, these derived charges are significantly smaller than those given by the Bader method. For instance, a point-charge analysis of core-ionization energy shifts in fluorobenzene³⁵ gives a charge of about +0.2 for the carbon to which the fluorine is attached, whereas the Bader approach³⁷ gives +0.47.

Our concern here is with two questions. First, to what extent does the point-charge model provide a realistic description of the charge distribution in a molecule and the potential at a given nucleus? Second, how is it possible to reconcile the rather large Bader charges with the relatively small shifts in core-ionization energy? We have previously reported experimental measurements and theoretical calculations of core-ionization energies for carbon in ethene and in the monohalogenated ethenes.³⁸ Our analysis of the point-charge model is based primarily on these compounds.

Computational Methods

Theoretical ionization energies have been determined by taking the difference between the calculated energies of the core-ionized and neutral molecules. Details of the theoretical methods are given below and the results for C(1) are summarized in Table II together with experimental core-ionization energies. The calculations are sufficiently accurate to reproduce the core-ionization energies within about 1 eV out of 300 and most of the shifts within a few hundredths of an eV. From these calculations we have derived values of ΔV for C(1) in each molecule relative to ethene. These are given in Table II. Also shown in this table are atomic charges based on Mulliken populations (MPA), natural orbital populations (NBO), and the Bader method (IBP).

The ionization energies were obtained by using MOLECULE-ALCHEMY³⁹ programs, which provide for the possibility of calculations on ions with a missing core electron. The basis sets were 3s for hydrogen,⁴⁰ 7s3p for carbon⁴¹ and fluorine,⁴¹ 10s6p for chlorine,⁴¹ 18s8p5d for bromine,⁴² and 25s11p7d for iodine.⁴³ These were contracted to double- ζ quality and augmented with a set of p functions on the hydrogen atoms and a set of d functions on the others.^{18,19}

The integrated Bader populations and potentials were obtained from the results of calculations with Gaussian86⁴⁴ with use of these basis sets. The code for calculating the natural orbital populations⁴⁵ was added to Gaussian82.⁴⁶ Since there appeared to be little difference between the charges from the Mulliken populations and those from natural orbital populations, the latter were not calculated for the bromine and iodine compounds.

All of the calculations were done with experimental geometries⁴⁷ except for fluoroethene, where only the optimized geometry could be run successfully by the Bader program. We use the following labeling conventions: the carbon to which the halogen is attached is C(1), the hydrogen attached to C(1) is H(4), and H(5) is trans to the halogen.

Bader populations were obtained from the PROAIMS program developed by Bader and co-workers.⁷ Their program was modified in two ways. First, a routine was added to calculate the electrostatic potential due to a basin at any external point by integrating ρ/r over the basin,

(36) (a) Thomas, T. D.; Weightman, P. *Phys. Rev. B* **1986**, *33*, 5406. (b) Holmes, S. A.; Thomas, T. D. *J. Am. Chem. Soc.* **1975**, *97*, 2337. (c) Shaw, R. W., Jr.; Carroll, T. X.; Thomas, T. D. *J. Am. Chem. Soc.* **1973**, *95*, 5870.

(37) Bader, R. W. F.; Chang, C. *J. Phys. Chem.* **1989**, *93*, 2946.

(38) Saethre, L. J.; Siggel, M. R. F.; Thomas, T. D. *J. Electron Spectrosc. Relat. Phenom.* **1989**, *49*, 119.

(39) The MOLECULE-ALCHEMY program package incorporates the MOLECULE integrals program written by J. Almlöf and the ALCHEMY programs written by P. Bagus, B. Liu, M. Yoshimine, and A. D. McLean, and modified by P. Bagus and U. Wahlgren.

(40) Huzinaga, S. *J. Chem. Phys.* **1965**, *42*, 1293.

(41) Roos, B.; Siegbahn, P. *Theor. Chim. Acta* **1970**, *17*, 209.

(42) Gropen, O. Unpublished results.

(43) Strömberg, A.; Gropen, O.; Wahlgren, U. *J. Comput. Chem.* **1983**, *4*, 181.

(44) Frisch, M. J.; Binkley, J. S.; Schlegel, H. B.; Raghavachari, K.; Melius, C. F.; Martin, R. L.; Stewart, J. J. P.; Bobrowicz, F. W.; Rohlfing, C. M.; Kahn, L. R.; DeFrees, D. J.; Seeger, R.; Whiteside, R. A.; Fox, D. J.; Fluder, E. M.; Pople, J. A. GAUSSIAN 86, Carnegie-Mellon University Publication Unit, Pittsburgh, Pennsylvania, 1984.

(45) We are grateful to Prof. Andrew Streitwieser, Jr., for the use of a computer code to calculate the natural populations. This code was obtained directly from Prof. Weinhold.

(46) Binkley, J. S.; Frisch, M. J.; DeFrees, D. J.; Krishnan, R.; Whiteside, R. A.; Schlegel, H. B.; Fluder, E. M.; Pople, J. A. GAUSSIAN 82, Carnegie-Mellon University Publication Unit, Pittsburgh, Pennsylvania, 1983.

(47) Callomon, J. H.; Hirota, E.; Kuchitsu, K.; Lafferty, W. J.; Maki, A. G.; Pote, C. S. *Landolt-Börnstein; Numerical Data and Functional Relationships in Science and Technology; New Series; Group II: Atomic and Molecular Physics; Structure Data of Free Polyatomic Molecules*; Hellwege, K.-H., Hellwege, A. M., Eds.; Springer-Verlag: Berlin, 1976; Vol. 7.

Table III. Theoretical Potentials Due to the Electrons in a Given Carbon Basin (V_N), Valence Electron Populations (N_v), and Average Inverse Radii of the Valence Electron ($(1/r)$)^a

X	C(1)			C(2)		
	V_N	N_v	$e(1/r)$	V_N	N_v	$e(1/r)$
H	-406.19	4.045	+24.13	-406.19	4.045	+24.13
F	-386.48	2.918	+26.70	-413.09	4.431	+23.59
Cl	-399.93	3.671	+24.88	-410.33	4.282	+23.76
Br	-402.48	3.856	+24.35	-410.38	4.288	+23.74
I	-405.96	4.104	+23.73	-409.25	4.214	+23.89

^a V_N and $e(1/r)$ are given in volts. C(1) is attached to halogen in haloethenes.

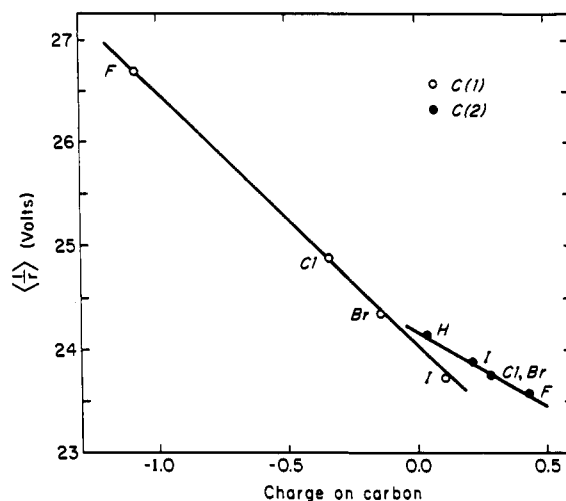


Figure 1. Potential due to a valence electron in the carbon basins in haloethenes as a function of basin charge. Open circles refer to the carbon to which the halogen is attached and closed circles to the other carbon.

where ρ is the charge density and r is the distance from the external point to a point within the basin. With this modification it is possible to calculate the contribution to the potential at any nucleus from any basin. Second, the program was modified to provide octupole moments of the basins. Algebraic expressions for these moments are given in the Appendix of this paper.

Failures of the Point-Charge Model

The haloethenes present a case in which the point-charge model gives the wrong answer.³⁸ The first column of numbers in Table II shows the ionization energies for C(1); the second column gives the theoretical values of the same quantities. Since there is good agreement between theory and experiment, we are confident that the theory can be used to calculate other quantities of interest, such as the potentials, which are given in the third column. These results show that the potential at C(1) in iodoethane is quite positive, even though the electronegativity of carbon is reported to be greater than that of iodine.⁴⁸

The last three columns of numbers in Table II shows charges on C(1) calculated from the three different methods. The first row shows the absolute values for ethene, and the other rows show the values relative to those for ethene. Although the charges from the different methods differ in detail, they are in agreement in the overall trend. The charge on C(1) is large and positive for fluoroethene, decreases rapidly as we move down the periodic table, and is negative for iodoethene. These results are in contrast to the values of ΔV , which decrease only slightly with increasing atomic number of the halogen, and remain distinctly positive relative to ethene.

In the simplest approximation, eq 2 is dominated by the first term and, therefore, we expect a relatively negative charge on the atom of interest to lead to a negative value of ΔV , and usually

(48) Cotton, F. A.; Wilkinson, G. *Advanced Inorganic Chemistry*, 3rd ed.; Interscience: New York, 1972; p 116.

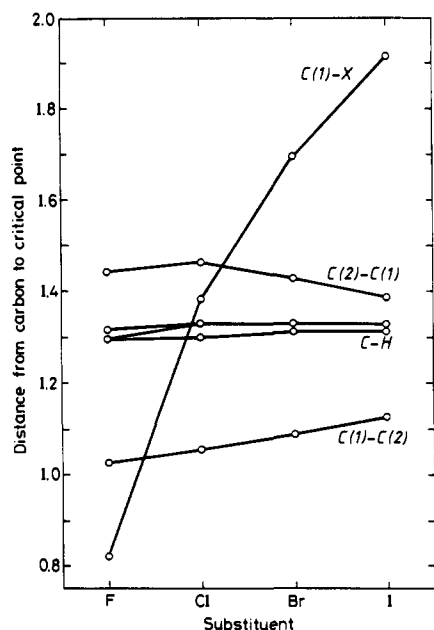


Figure 2. Distance from carbon atoms to bond critical points for haloethenes.

to a negative value of ΔI . The remaining terms, which sum to the Madelung potential, have opposite sign to the leading term, but in no case are they large enough to offset the dominance of the leading term and reverse the sign of the shift. The results just mentioned, especially those for iodoethene, are therefore in disagreement with the predictions of the point-charge model.

Where does this failure of the point-charge model arise? Two essential assumptions of the model described by eq 2 are that the valence radius is a constant, independent of atomic charge and molecular composition, and that the charges on the surrounding atoms can be treated as points centered at the nuclei. We consider each of these below.

The Valence Radius. The assumption that $\langle 1/r_i \rangle$ is independent of the charge on the atom of interest is certainly not valid; the valence radius increases with increasing number of valence electrons. The Bader analysis provides a method for assessing the importance of this effect. From the charge-density integrations we can obtain that part of the potential that is due to electrons in the basins of interest. This potential can be written as

$$V_N = -\sum_k N_k \left\langle \frac{1}{r} \right\rangle_k \quad (3)$$

where N_k is the number of electrons in orbital k and $\langle 1/r \rangle_k$ is the expectation value of $1/r$ for this orbital. Most of the potential is due to the inner-shell electrons, carbon 1s in this case. Removing this contribution with use of atomic inner-shell wave functions⁴⁹ gives the contribution from the valence electrons, $N_{\text{val}} \langle 1/r \rangle_{\text{val}}$. From this and the valence population we obtain $\langle 1/r \rangle$ for the valence electrons of carbon in each of these compounds. The results are summarized in Table III and in Figure 1. We see the expected decrease in $\langle 1/r \rangle$ as the valence population increases. However, this is not the only effect, since the variation of $\langle 1/r \rangle$ with population is about twice as great for C(1) as for C(2). The effective value of $\langle 1/r \rangle$ depends not only on the valence population but also on the nature of the other atoms to which the atom of interest is attached.

Although the increase in valence radius (decrease in $\langle 1/r \rangle$) with increasing valence population is readily understood, the effect of substituent on valence radius, reflected in the different slopes of the lines in Figure 1, was not expected. Inspection of the bond critical points of the Bader basins (points of minimum electron density along the bond directions) reveals the reasons for this effect. In Figure 2 we show the position of the bond critical point for

the different halogenated species. For the most part, the C(2) basin size is independent of the halogen. For this basin $\langle 1/r \rangle$ is determined by the total number of electrons in the basin—the greater this number, the more the electrons will spread to the periphery of the basin and the smaller will be $\langle 1/r \rangle$. For C(1), however, there is an additional effect: the size of the basin in the C(1)-X direction increases markedly with increasing size of the halogen and, hence, with the number of electrons in the basin. These electrons can spread over a larger volume than is available around C(2), and $\langle 1/r \rangle$ decreases more rapidly with increasing number of electrons than does $\langle 1/r \rangle$ for C(2).

For neutral carbon, the two lines drawn in Figure 1 give a value of $\langle 1/r \rangle$ between 24.1 and 24.2 V. These are between the atomic values for 2s and 2p on carbon of 24.4 and 21.3 V,⁵⁰ respectively. In addition, the slopes in Figure 1 are -2.4 V/electron for C(1) and -1.4 V/electron for C(2), which are not far from those for a free carbon atom, -2.9 V/electron for 2p and -1.5 V/electron for 2s.⁵⁰ Thus, these results of the Bader integration are in reasonable accord with the results of atomic calculations.

The Extraatomic Potential in the Point-Charge Approximation. The potential at the atom of interest is determined not only by the charge on the atom of interest but also on the potential due to the charge distribution on the other atoms—the extraatomic potential. We distinguish between the “extraatomic” potential, which is the actual potential due to the surrounding atoms, and the “Madelung” potential, which is the potential due to an assembly of point charges located at the atomic centers.

The second assumption of the point-charge model is that the charges on atoms other than the one of interest can be treated as if they are point charges located at the nuclei. In this case, the extraatomic potential and the Madelung potential are equal, and the potential due to any atom j at any center i is given by q_j/R_{ij} , as indicated in eq 2. The values of R_{ij} are all known and the integration of ρ/r for each Bader basin gives the correct values of these potentials. From these it is possible to calculate effective values of q_j for each basin. For the haloethenes each basin produces potentials at five other atoms and these potentials yield five independent values of the charge for that basin. If the assumptions of the point-charge model are correct, then these values should all agree with one another and should agree with the integrated Bader charge for that basin.

An application of this approach to fluoro- and bromoethene is shown in Table IV. Here each row represents one of the basins. The entries in that row give the values of the effective charge for that basin derived from the potentials produced by that basin at the atoms indicated at the heads of the columns. The integrated Bader charges are given in the next-to-last column.

For fluoroethene the results are, in general, plausible. The worst discrepancies are for the charge at C(2) derived from the potentials that it produces at H(5) and H(6). The effect of a nonspherical electron distribution about C(2) will be felt most at the nearest atoms, which are H(5) and H(6). If we omit consideration of numbers that arise from the potential due to adjacent basins, all of the remaining values are reasonable. The average value of the remaining effective charges is shown in the last column of Table IV. These compare reasonably well with the Bader charges and give a total charge on the molecule of +0.05, which, though not equal to zero, is close to it.

However, when we consider the charges in bromoethene, we see that they do not agree at all well with the integrated Bader charges. Even if we eliminate the contribution from adjacent basins, the agreement is still not good. For C(1), the average charge is twice the Bader charge, and for bromine the derived charge is of opposite sign to the Bader charge. The sum of the average charges is 0.36, which is far from zero.

This test of the point-charge model, which works reasonably well for fluoroethene, fails badly for bromoethene. The likely reason for the success is that fluoroethene is a highly polar molecule, with large charges. The potentials are dominated by

(49) Desclaux, J. P. *At. Data Nucl. Data Tables* 1973, 12, 312.

(50) Calculated from wave functions given by: Clementi, E.; Roetti, C. *At. Data Nucl. Data Tables* 1974, 14, 312.

Table IV. Derived Values of Effective Atomic Charge from Theoretical Potentials Due to the Electrons in a Given Basin and Internuclear Distance^a

charge on atom	center at which charge is calculated						IBP ^b	av ^c
	C(1)	C(2)	X(3)	H(4)	H(5)	H(6)		
Fluoroethene								
C(1)	-	+1.268	+1.484	+1.000	+1.086	+1.209	+1.082	+1.148
C(2)	-0.396	-	-0.451	-0.418	-0.044	-0.054	-0.431	-0.435
F(3)	-0.960	-0.875	-	-0.964	-0.852	-0.835	-0.778	-0.882
H(4)	+0.144	+0.083	+0.091	-	+0.063	-	+0.053	+0.079
H(5)	+0.069	+0.126	+0.057	+0.044	-	+0.075	+0.033	+0.061
H(6)	+0.083	+0.139	+0.058	+0.072	+0.087	-	+0.045	+0.075
Bromoethene								
C(1)	-	+0.481	+0.158	+0.299	+0.295	+0.294	+0.144	+0.295
C(2)	-0.201	-	-0.284	-0.263	+0.038	+0.029	-0.288	-0.274
Br(3)	+0.306	+0.098	-	+0.135	+0.051	+0.022	-0.052	+0.077
H(4)	+0.180	+0.117	+0.120	-	+0.097	+0.112	+0.090	+0.112
H(5)	+0.044	+0.141	+0.069	+0.060	-	+0.089	+0.048	+0.066
H(6)	+0.052	+0.156	+0.073	+0.088	+0.105	-	+0.053	+0.080

^aThe charges given by the IBP method are also given for comparison. C(1) is attached to the halogen, H(4) is attached to C(1), and H(5) is trans to the halogen. ^bIBP is from integrated Bader population analysis. ^cThe average charge when numbers from adjacent basins are omitted. See text.

these charges and the effects of nonspherical charge distributions are small compared with the effects of charge alone. The likely reason for the failure is the reverse. Bromoethene is not strongly polar and the charges play only a small role in determining the potentials, which are, in fact, largely determined by higher moments of the charge distribution in each basin (see below).

It is apparent from the foregoing analysis that the assumption of point charges is not satisfactory and that a more complete model of the charge distribution is needed. Such a model is considered in the following section.

The Multipole Model

The assumption that the atomic charges can be treated as points is equivalent to assuming that the charge assigned to a given atom is spherically distributed about its nucleus. This is not the case for two reasons. First, it is impossible to divide a region of space into nonoverlapping spheres that fill all of the space—some of the volumes must be nonspherical. Second, even if the charge distribution in the isolated atom is spherical, the overlap of wave functions in the molecule leads to buildup of electron density in the bond between the atoms and depletion of electron density away from the bond. Even for a homonuclear diatomic molecule the potential is shifted from that in the free atom because of this neighboring dipole. For example, in H₂ the potential at the proton is nearly 3 V more negative than it is in the H atom.⁵¹ If there is significant charge transfer between two atoms, then the atomic charges influence the moments on the adjacent atoms. The net effect for polar bonds is that the centers of charge on the adjacent atoms are closer together than the two nuclei. For molecules with incompletely filled p orbitals there will be quadrupole moments that may be large.

An important consequence of the nonspherical charge distribution is that the point-charge model may predict a shift in V that is too large for a given set of atomic charges, or, conversely, if the model is used to derive atomic charges for measured shifts, these charges will be too small. This effect can be seen by considering ΔV for polar molecules of the type AX_n, where A is the central atom and X is an electronegative ligand. The shift relative to a neutral A can be expressed as³⁴

$$\Delta V_A = q_A \left(\left\langle \frac{1}{r_A} \right\rangle - \frac{1}{R_{AX}} \right) \quad (4)$$

Because the positive charge on A polarizes the electrons on X toward A, the distance between the center of charge on X and the nucleus of atom A is less than R_{AX} . Therefore, the term in parentheses will be too large if we use the internuclear distance and the predicted value of the shift will be too large (or the derived value of the charge too small). This effect can produce the

Table V. Atomic Multipole Contributions to the Potentials at C(1) in Ethene^a

atom	$V_N + V_q$	V_μ	V_Q	V_o	V_{sum}	V_{num}
C(1)	-406.19	0.00	0.00	0.00	-406.19	-406.19
C(2)	-0.49	0.30	1.72	1.47	3.00	1.80
H(3)	0.29	0.85	0.79	-0.42	1.51	1.54
H(4)	0.29	0.85	0.79	-0.42	1.51	1.54
H(5)	0.15	0.20	0.06	-0.01	0.39	0.39
H(6)	0.15	0.20	0.06	-0.01	0.39	0.39
total	-405.81	2.40	3.42	0.61	-399.38	-400.52

^aThe theoretical potentials due to the electrons in a given basin are given for comparison. All values in volts. V_N = potential due to the electrons on C(1). V_q = potential due to the charge, or Madelung potential, from atoms 2-6. V_μ = potential due to the dipole contribution from atoms 2-6. V_Q = potential due to the quadrupole contribution from atoms 2-6. V_o = potential due to the octupole contribution from atoms 2-6. $V_{sum} = V_N + V_q + V_\mu + V_Q + V_o$. V_{num} = potential calculated from numerical integration over each basin.

apparent discrepancies between the large charges of the Bader approach and the small shifts in core-ionization energies.

The consequences of the nonspherical distribution of charge about the nuclei can be illustrated by replacing the point-charge model, eq 2, with a point-multipole model. The potential at some point i can be described by the multipole expansion⁵²

$$V_i = -\sum_k N_{ik} \left\langle \frac{1}{r_i} \right\rangle_k + \sum_j \frac{q_j}{R_{ij}} + \sum_j \frac{\vec{\mu}_j \cdot \vec{R}_{ij}}{R_{ij}^3} + \frac{1}{2} \sum_j \frac{\vec{R}_{ij} \cdot \vec{Q}_j \cdot \vec{R}_{ij}}{R_{ij}^5} + \text{octupole and higher terms} \quad (5)$$

N_{ik} is the number of electrons in the k th atomic orbital of the atom of interest and $\langle 1/r_i \rangle_k$ is the appropriate expectation value for the same orbital. The first sum goes over these orbitals and the other sums go over the other atoms in the molecule, j . The distance between atom i and atom j is represented by R_{ij} , the charge on j by q_j , the dipole moment vector by $\vec{\mu}_j$, and the quadrupole moment tensor by \vec{Q}_j . The expression for the octupole term is given in the Appendix. The multipole moments for each atomic basin can be obtained from the Bader integrations and give the potential at the center of interest due to the other atoms. If the expansion is carried out to convergence, this potential is equal to the extraatomic potential discussed earlier. This is in distinction to the Madelung potential, which includes only the second term of eq 5.

Using this approach, we have calculated the contribution of each basin multipole to the potential at each atomic center in the monohaloethenes, including multipoles up to the octupole moment. The potential at an atom due to the charge distribution in its own

(51) Calculated with the 6-31G** basis set.

(52) Condon, E. U. In *Handbook of Physics*, 2nd ed.; Condon, E. U., Odishaw, H., Eds.; McGraw-Hill: New York, 1967; pp 4-17.

Table VI. Atomic Multipole Contributions to the Potential Shift at C(1) for Haloethenes Relative to Ethene^a

X	ΔV_N	ΔV_q	ΔV_μ	ΔV_Q	ΔV_o	ΔV_{sum}	ΔV_{num}	ΔV_{anal}
Individual Contributions								
H	0.00	0.00	0.00	0.00	0.00	0.00	0.00	0.00
F	+19.71	-12.32	-4.64	-1.07	+0.90	+2.59	+2.46	+2.39
Cl	+6.26	-3.52	-1.43	+0.12	+0.61	+2.04	+2.04	+1.99
Br	+3.71	-1.92	-0.97	+0.29	+0.73	+1.84	+1.89	+1.79
I	+0.24	+0.14	+0.05	+0.81	+0.58	+1.82	+1.77	+1.69
Sum								
H	0.00	0.00	0.00	0.00	0.00	0.00	0.00	0.00
F	+19.71	+7.40	+2.76	+1.69	+2.59	+2.59	+2.46	+2.39
Cl	+6.26	+2.74	+1.31	+1.43	+2.04	+2.04	+2.04	+1.99
Br	+3.71	+1.80	+0.82	+1.12	+1.84	+1.84	+1.89	+1.79
I	+0.24	+0.38	+0.43	+1.24	+1.82	+1.82	+1.77	+1.69

^a All values in volts. The symbols V_N , V_q , V_μ , V_Q , and V_o are defined in Table V. $\Delta V_{\text{sum}} = \Delta V_N + \Delta V_q + \Delta V_\mu + \Delta V_Q + \Delta V_o$. ΔV_{num} = potential shift calculated from numerical integration over each basin. ΔV_{anal} = potential shift calculated from analytic integration of the wave function and given directly by the G86 program.

basin is obtained by integrating ρ/r over the basin (ρ is the charge density). Thus the effect of variation of $\langle 1/r \rangle$ with charge and neighboring atoms is correctly included.

Absolute Potentials. An illustration of the multipole model is shown in Table V, where we present the contributions from the different multipoles to the potential at C(1) in ethene. We see that the higher multipoles play an important role in establishing this potential. The total contribution to the extraatomic potential from point charges is small since the charges on the atoms are small ($q_C = -0.045$, $q_H = +0.022$). Most of the extraatomic potential comes from the higher multipoles. The effect of the adjacent carbon basin, C(2), is especially noticeable, and the multipole expansion for this basin does not give the correct value even when carried out to the octupole term. For H(3) and H(4), although the expansion gives the correct value, the contributions from the octupole terms are not small. It is apparent that the multipole expansion does not converge rapidly. The large magnitude of the higher multipole components in the Bader partitioning has also been noted by Stone and Alderton,⁵³ who pointed out that any partitioning into nonoverlapping volumes will lead to large higher moments.

The extent to which the multipole expansion has converged can be seen from a comparison of the last two columns in Table V. The first of these shows the sum of the multipole terms and the second the potential obtained by numerical integration of ρ/r over the basin. We see that there is good agreement except for the contribution from the adjacent carbon basin. The multipole expansion gives a contribution of 3.0 V from C(2) and C(1), whereas numerical integration gives only 1.80 V. The C(2) basin has a distorted charge distribution and is close to C(1); such a failure of the multipole expansion under these circumstances is not unexpected.

The haloethenes show essentially the same behavior as ethene. The multipole expansion carried through the octupole term gives a reasonably accurate value of the potential except for contributions from carbon to an adjacent atom. For the potential at the halogen this error diminishes as the carbon-halogen bond gets longer, since the next term in the multipole expansion falls off as the fifth power of the distance. For iodoethene the potential at the iodine atom calculated from the multipole expansion is within 0.13 V of that obtained from analytical integration of the wave function.

Relative Potentials. We now consider the contributions of the different multipoles to the shifts in potential for carbon in haloethenes relative to carbon in ethene. Table VI shows the results for C(1); the upper part gives the contributions of each moment separately and the lower part the cumulative sum for all of the moments up to a given moment. The first column of numbers gives the value of $\Delta(N_i \langle 1/r \rangle)$, that is, the contribution to the shift from the charge on C(1). The next four columns show the contributions from the various multipoles of the surrounding basins. For comparison, the last two columns give the shifts obtained from

integration of the actual charge density. The next-to-last column gives the results of numerical integration over the basins and the last column the results of analytical integration of the wave functions. These two methods should agree exactly with each other. The discrepancies between the two methods of less than 0.1 V reflect the inaccuracies of the Bader integration procedure. Comparing the last two columns with the sums of the multipole terms shows that the multipole expansion carried to this point agrees with the exact values, but using fewer terms is not satisfactory. It is to be noted that the octupole contributions to the shift are by no means small, and it is not certain that the expansion has converged even when applied to shifts.

In Table VI we see a number of the effects that have been discussed earlier. For iodoethene, the part of ΔV that is due to the charge on C(1), ΔV_N , is positive, even though Δq is negative; this is the result of the variation of $\langle 1/r \rangle$ with substituent that has been discussed previously. For the other three compounds this shift is also positive, but the Madelung contribution from the other atoms is negative, in keeping with the positive charge on C(1) (and equal negative charge on the rest of the molecule) and the usual point-charge model. However, for the most polar molecules, fluoro- and chloroethene, the combined effect of these point-charge terms is significantly larger than the total shift. Charges derived for these compounds from the actual shift by using the standard point-charge model, eq 2, will, therefore, be too small. For iodoethene the total contribution from the higher multipoles is considerably greater than that from the Madelung potential, with that from the quadrupole especially important. Thus ΔV for iodoethene has no simple relationship to the charge on C(1).

Different Choices of Boundaries. For the more polar systems considered here, such as fluoro- and chloroethene, a different choice of basin boundaries would lead to rather different results. If the C(1) boundaries are enlarged, then the atomic charges and monopole terms calculated from the integrations will be smaller. The dipole terms will also be smaller, since negative charge on the periphery of the halogen basin will have been transferred to the C(1) basin. However, such a procedure would involve a totally arbitrary definition of the basin, whereas the Bader method provides a well-defined procedure for selecting the basin boundaries on the basis of the charge density. The use of Bader's atomic basin boundaries may, on the other hand, enhance the relative importance of multipole components higher than dipole relative to other partitioning methods.⁵³

The partitioning scheme proposed by Stone and Alderton⁵³ and by Vign -Maeder and Claverie⁵⁴ uses overlapping charge distributions centered at a number of points in the molecule. Typically these points are chosen as the atomic centers and the midpoints of the bonds. This procedure has the advantage of giving a more rapidly converging multipole expansion but also the disadvantage of giving results that are basis-set dependent.⁵³

For homonuclear diatomic molecules there is no ambiguity about either the atomic charges (zero) or the basin boundary (the

(53) Stone, A. J.; Alderton, M. *Mol. Phys.* **1985**, *56*, 1047.(54) Vign -Maeder, F.; Claverie, P. *J. Chem. Phys.* **1988**, *88*, 4934.

Table VII. Atomic Multipole Contributions to the Potential Shift at X(1) for Diatomic Halogens^a

X ₂	V _μ	V _Q	V _o	V _{sum}	V _{num}
Cl ₂	0.51	1.14	0.07	1.72	1.67
Br ₂	0.26	0.87	0.06	1.19	1.15
I ₂	0.30	0.85	0.03	1.17	1.16

^aAll values in volts. V_μ = potential due to the dipole contribution. V_Q = potential due to the quadrupole contribution. V_o = potential due to the octupole contribution. V_{sum} = V_μ + V_Q + V_o. V_{num} = potential calculated from numerical integration over each basin.

mirror plane perpendicular to the molecular axis). The effects of the basin moments on the potentials for Cl₂, Br₂, and I₂ are given in Table VII, where we see that the nonspherical charge distribution on one halogen produces a significant potential at the other. Redefining the basins to be overlapping spheres might minimize these moments, but it would not eliminate them. The redistribution of charge along the bond axis produces a dipole moment for each basin. Quadrupole moments arise because the p orbitals are not completely filled. For the dihalogens, in which the pσ orbital contains only 1 electron, the quadrupole contribution is particularly significant.

Conclusions

We see that the fundamental assumptions of the point-charge model are wrong. The valence radius depends on both valence population and molecular composition. The charges on atoms away from the atom of interest cannot be treated as point charges. The latter effect is particularly important for molecules of low polarity, where the extraatomic potential can be dominated by the higher multipoles of the charge distributions.

The multipole expansion provides a way for understanding these effects, but it converges slowly. For absolute potentials there can be significant discrepancies between the results of the multipole expansion and the exact results even when the expansion is carried through the octupole term. For shifts, there is reasonably good agreement between the results of the multipole expansion and the exact results, but even here, there is reason to question whether the expansion has converged by the octupole term.

Acknowledgment. This work was supported in part by the U.S. National Science Foundation, the U.S. Department of Energy, and the Norwegian Research Council for Science and the Humanities. We are indebted to Andrew Streitwieser, Jr., for providing computer facilities for some of the calculations, to Richard Bader for a copy of his program and for his permission to modify it, and to one of the referees for bringing to our attention the work of Stone and Alderton and Vigné-Maeder and Claverie. M.R.F.S. thanks David A. Shirley, the Norwegian Council for Scientific and Industrial Research, and the Norwegian Marshall Fund for support.

Appendix

The PROAIMS program calculates the number of electrons and other quantities associated with the electron distribution in a given region of space. In this study, each region contained one nucleus and the electron distribution assigned to that nucleus. All desired quantities were calculated by dividing the total volume of a region into small volume elements with use of spherical polar coordinates with the origin at the nucleus; summation was then carried out over φ, θ, and r.

General expressions for the moments of a charge distribution and the potential due to these moments at an arbitrary position

are given by Condon.⁵² There are seven independent octupole moments. For our purposes, it was most convenient to express these in Cartesian coordinates, and we have converted the expressions given by Condon accordingly. We have used the following algebraic expressions for the seven octupole moments

$$O_{xxx} = \sum_{\phi} \left\{ \sum_{\theta} \left[\sum_r -\rho * (x^3 - 3xy^2) * w_r \right] w_{\theta} \right\} w_{\phi}$$

$$O_{xyz} = \sum_{\phi} \left\{ \sum_{\theta} \left[\sum_r -\rho * (2xyz) * w_r \right] w_{\theta} \right\} w_{\phi}$$

$$O_{zxx-zyy} = \sum_{\phi} \left\{ \sum_{\theta} \left[\sum_r -\rho * (zx^2 - zy^2) * w_r \right] w_{\theta} \right\} w_{\phi}$$

$$O_{yyy} = \sum_{\phi} \left\{ \sum_{\theta} \left[\sum_r -\rho * (3yx^2 - y^3) * w_r \right] w_{\theta} \right\} w_{\phi}$$

$$O_{xzz} = \sum_{\phi} \left\{ \sum_{\theta} \left[\sum_r -\rho * (5xz^2 - xR^2) * w_r \right] w_{\theta} \right\} w_{\phi}$$

$$O_{yzz} = \sum_{\phi} \left\{ \sum_{\theta} \left[\sum_r -\rho * (5yz^2 - yR^2) * w_r \right] w_{\theta} \right\} w_{\phi}$$

$$O_{zzz} = \sum_{\phi} \left\{ \sum_{\theta} \left[\sum_r -\rho * (\frac{5}{3}z^3 - zR^2) * w_r \right] w_{\theta} \right\} w_{\phi}$$

where R is the distance from the nucleus to the point where the electron density, ρ, is being determined, and x, y, z are the Cartesian and r, θ, and φ the spherical coordinates of this point relative to the nucleus. The quantities w_r, w_θ, and w_φ are weighting factors and incorporate the dimensions of the small finite volume element in which the charge density is calculated, normalization parameters, and conversion factors. The central parts of the equations given above (omitting the weighting factors and the summations) were added to the subroutine FUNC in the PROAIMS program.

The octupole contribution to the potential at a given nucleus was calculated by combining the octupole moments with use of the equation

$$V_o = \sum_i \left\{ \frac{9}{4} (\frac{5}{3}z_i^3 - z_i R_i^2) O_{zzz_i} + \frac{3}{8} (5z_i^2 - R_i^2) \right. \\ \left. (x_i O_{xzz_i} + y_i O_{yzz_i}) + \frac{15}{4} [z_i (x_i^2 - y_i^2) O_{zxx-zyy_i} + 2x_i y_i z_i O_{xyz_i}] + \right. \\ \left. \frac{5}{8} [(x_i^3 - 3x_i y_i^2) O_{xxx_i} + (3x_i^2 y_i - y_i^3) O_{yyy_i}] \right\} R_i^{-7}$$

where the sum is over all the other nuclei in the molecule. The quantities R_i are the distances between the nucleus of interest and the other nuclei, and x_i, y_i, z_i are the Cartesian coordinates of the other nuclei relative to the one of interest.

The octupole moments given above are actually not the moments defined by Condon,⁵² nor are they the true octupole moments of the distribution. Condon defines the multipole moments in terms of normalized spherical harmonics, with the result that some of the moments are complex. We have used appropriate linear combinations to give real moments. In addition, we have not included in these moments a factor of 4π/7 that appears in Condon's expressions because of his use of normalized spherical harmonics. In the complete calculation of moments and potential, this is cancelled by the two factors of √7/4π that appear in the normalization of the spherical harmonics. Finally, some constant numerical factors that are part of the definition of the moments have not been included in our moments, but have been combined with similar factors in the calculation of the potential. To obtain a consistent set of real octupole moments, the seven expressions given above should be multiplied by 3/2, √3/8, √3/8, √15/4, √15/4, √5/8, and √5/8, respectively. If these moments are used, then these same factors should replace the fractions given in the expression for the potential.